

# Formation and Dynamics of Dark Solitons and Vortices in Quantum Electron Plasmas

P. K. Shukla and B. Eliasson

*Institut für Theoretische Physik IV, Ruhr-Universität Bochum, D-44780 Bochum, Germany*

(Received 23 March 2006; published 20 June 2006)

We present simulation studies of the formation and dynamics of dark solitons and vortices in quantum electron plasmas. The electron dynamics in the latter is governed by a pair of equations comprising the nonlinear Schrödinger and Poisson system of equations, which conserves the number of electrons as well as their momentum and energy. The present governing equations in one spatial dimension admit stationary solutions in the form a dark envelope soliton. The dynamics of the latter reveals its robustness. Furthermore, we numerically demonstrate the existence of cylindrically symmetric two-dimensional quantum electron vortices, which survive during collisions. The nonlinear structures presented here may serve the purpose of transporting information at quantum scales in ultracold micromechanical systems and dense plasmas, such as those created during intense laser-matter interactions.

DOI: [10.1103/PhysRevLett.96.245001](https://doi.org/10.1103/PhysRevLett.96.245001)

PACS numbers: 52.35.Sb, 71.10.Ca

Quantum plasmas are ubiquitous in micromechanical systems and ultrasmall electronic devices [1], in laser and microplasmas [2], and in dense astrophysical environments [3]. In such plasmas, quantum mechanical effects (e.g., tunneling) are important since the de Broglie length of the charge carriers (e.g., electrons and holes or positrons) is comparable to the dimension of the system. Recently, there has been a growing interest [4–9] in investigations of relevant quantum hydrodynamic (QHD) models for charged particle systems and collective interactions in quantum plasmas. The QHD model has been introduced to deal with negative differential resistance and resonant tunneling phenomena in microelectronic devices [10]. Quantum transport models, similar to the QHD plasma models, have also been used in superfluidity [11] and superconductivity [12], as well as in the study of metal clusters and nanoparticles, where they are referred to as nonstationary Thomas-Fermi models [13].

In this Letter, we investigate, by means of computer simulations, the formation and dynamics of dark or gray envelope solitons and vortices in quantum electron plasmas with fixed ion background. The results are relevant for the transport of information at quantum scales in microplasmas as well as in micromechanical systems and microelectronics. For our purposes, we shall use an effective Schrödinger-Poisson model [4–7], which was developed by employing the Wigner-Poisson phase space formalism on the Vlasov equation coupled with the Poisson equation for the electric potential. Such a model was originally derived by Hartree in the context of atomic physics for studying the self-consistent effect of atomic electrons on the Coulomb potential of the nucleus.

Generalizing the one-dimensional Schrödinger-Poisson system of equations [5] to  $D$  dimensions, we have

$$i \frac{\partial \Psi}{\partial t} + A \nabla^2 \Psi + \varphi \Psi - |\Psi|^{4/D} \Psi = 0, \quad (1)$$

and

$$\nabla^2 \varphi = |\Psi|^2 - 1, \quad (2)$$

where the wave function  $\Psi$  is normalized by  $\sqrt{n_0}$ , the electrostatic potential  $\varphi$  by  $T_F/e$ , the time  $t$  by  $\hbar/T_F$ , and the space  $\mathbf{r}$  by  $\lambda_D$ . We have introduced the notations  $\lambda_D = (\epsilon_0 T_F / n_0 e^2)^{1/2}$  and  $A = \Gamma_Q / 2$ , where the quantum coupling parameter  $\Gamma_Q = m e^2 / \hbar^2 \epsilon_0 n_0^{1/3}$  can be both smaller and larger than unity for typical metallic electrons [5]. Here  $n_0$  is the equilibrium electron number density,  $T_F \sim \hbar^2 n_0^{2/3} / m_e$  is the Fermi temperature (neglecting irrelevant dimensionless constant),  $m_e$  is the electron mass,  $e$  is the magnitude of the electron charge,  $\epsilon_0$  is the electric permittivity, and  $\hbar$  is the Planck constant divided by  $2\pi$ . The system of Eqs. (1) and (2) is supplemented by the Ampère law  $\partial \mathbf{E} / \partial t = iA(\Psi \nabla \Psi^* - \Psi^* \nabla \Psi)$ , where the electric field  $\mathbf{E} = -\nabla \varphi$ . Equations (1) and (2) conserve the number of electrons  $N = \int |\Psi|^2 d^3x$ , the electron momentum  $\mathbf{P} = -i \int \Psi^* \nabla \Psi d^3x$ , the electron angular momentum  $\mathbf{L} = -i \int \Psi^* \mathbf{r} \times \nabla \Psi d^3x$ , and the total energy  $\mathcal{E} = \int [-\Psi^* A \nabla^2 \Psi + |\nabla \varphi|^2 / 2 + |\Psi|^{2+4/D} D / (2+D)] d^3x$ . We note that a one-dimensional version of Eq. (1) without the  $\varphi$  term has also been used to describe the behavior of a Bose-Einstein condensate [14].

Let us first consider a quasistationary, one-dimensional ( $D = 1$ ) structure moving with a constant speed  $v_0$ , and make the ansatz  $\Psi = W(\xi) \exp(iKx - i\Omega t)$ , where  $W$  is a complex-valued function of the argument  $\xi = x - v_0 t$ , and  $K$  and  $\Omega$  are a constant wave number and frequency shift, respectively. By the choice  $K = v_0 / 2A$ , we can then write Eqs. (1) and (2) in the stationary frame as

$$\frac{d^2 W}{d\xi^2} + \lambda W + \frac{\varphi W}{A} - \frac{|W|^4 W}{A} = 0, \quad (3)$$

and

$$\frac{d^2 \varphi}{d\xi^2} = |W|^2 - 1, \quad (4)$$

where  $\lambda = \Omega/A - v_0^2/4A^2$  is an eigenvalue of the system. From the boundary conditions  $|W| = 1$  and  $\varphi = 0$  at  $|\xi| = \infty$ , we determine  $\lambda = 1/A$  and  $\Omega = 1 + v_0^2/4A$ . The system of Eqs. (3) and (4) admits a first integral

$$H = A \left| \frac{dW}{d\xi} \right|^2 - \frac{1}{2} \left( \frac{d\varphi}{d\xi} \right)^2 + |W|^2 - \frac{|W|^6}{3} + \varphi |W|^2 - \varphi - \frac{2}{3} = 0, \quad (5)$$

where we have used the boundary conditions  $|W| = 1$  and  $\varphi = 0$  at  $|\xi| = \infty$ .

We have solved Eqs. (3) and (4) numerically and have presented the results in Fig. 1. Here we have plotted the profiles of  $W^2$  and  $\varphi$  for a few values of  $A$ , where  $W$  was set to  $-1$  on the left boundary and to  $+1$  on the right boundary; i.e., the phase shift is  $180^\circ$  between the two boundaries. We see that we have solutions in the form of a dark soliton, with a localized depletion of the electron density  $N_e = |W|^2$ , and where  $W$  has different sign on different sides of the solitary structure. The local depletion of the electron density is associated with a positive potential. Larger values of the parameter  $A$  give rise to larger amplitude and wider dark solitons. Unlike a dark soliton associated with the usual cubic Schrödinger equation in which the group dispersion and the nonlinearity coefficient have opposite sign, the modulus of the wave function in the present work has localized maxima on both sides of the density depletion. If the boundary conditions are shifted below  $180^\circ$  (i.e., by a complex number), we could have a ‘‘gray soliton,’’ which is characterized by a nonzero density at the center of the soliton. In order to assess the dynamics and stability of the dark soliton, we have solved the time-dependent system of Eqs. (1) and (2) numerically with  $D = 1$ , and have displayed the result in Fig. 2. The

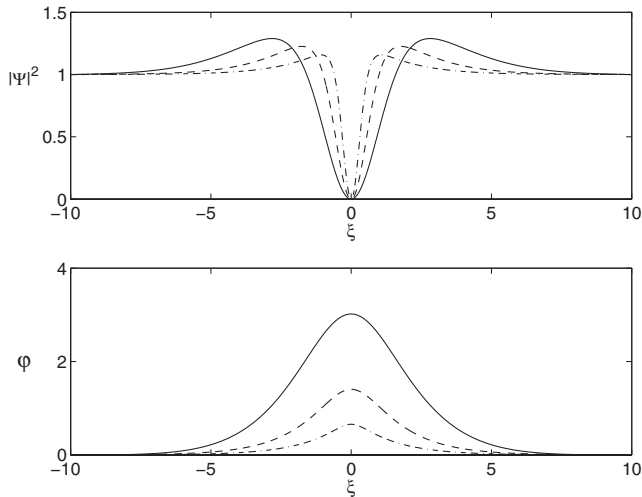


FIG. 1. The electron density  $|\Psi|^2$  (upper panel) and electrostatic potential  $\varphi$  (lower panel) associated with a dark soliton supported by the system of Eqs. (3) and (4), for  $A = 5$  (solid lines),  $A = 1$  (dashed lines), and  $A = 0.2$  (dash-dotted lines).

initial condition is  $\Psi = 0.18 + \tanh[20 \sin(x/10)] \times \exp(iKx)$ , where  $K = v_0/2A$ ,  $A = 5$ , and  $v_0 = 5$ . We clearly see oscillations and wave turbulence in the time-dependent solution presented in Fig. 2. Two very clear and long-lived dark solitons are visible, associated with a positive potential of  $\varphi \approx 3$ , which is consistent with the quasi-stationary solution of Fig. 1 for  $A = 5$ . Hence, the dark solitons seem to be robust structures that can withstand perturbations and turbulence during a considerable time.

We next consider two-dimensional ( $D = 2$ ) vortex structures of the form  $\Psi = \psi(r) \exp(in\theta - i\Omega t)$ , where  $r$  and  $\theta$  are the polar coordinates defined via  $x = r \cos(\theta)$  and  $y = r \sin(\theta)$ ,  $\Omega$  is a constant frequency shift, and  $n = 0, \pm 1, \pm 2, \dots$ , for different excited states (charge states). With this, we can write Eqs. (1) and (2) in the form

$$\Omega \psi + A \left( \frac{d^2}{dr^2} + \frac{1}{r} \frac{d}{dr} - \frac{n^2}{r^2} \right) \psi + \varphi \psi - |\psi|^2 \psi = 0, \quad (6)$$

and

$$\left( \frac{d^2}{dr^2} + \frac{1}{r} \frac{d}{dr} \right) \varphi = |\psi|^2 - 1, \quad (7)$$

respectively, where the boundary conditions  $\psi = 1$  and  $\varphi = d\psi/dr = 0$  at  $r = \infty$  determine  $\Omega = 1$ . Different signs of  $n$  represent different rotation directions of the vortex. For  $n \neq 0$ , we must have  $\psi = 0$  at  $r = 0$ , and from symmetry considerations we have  $d\varphi/dr = 0$  at  $r = 0$ . In Fig. 3, we display numerical solutions of Eqs. (6) and (7) for different charge states  $n$  and for  $A = 5$ . We see that the vortex is characterized by a complete depletion of the electron density at the core of the vortex and is associated with a positive electrostatic potential. Vortices with higher charge states are wider and are associated with a larger potential. In order to assess the stability of the vortices, we have numerically solved the time-dependent system of Eqs. (1) and (2) in two-space dimensions ( $D = 2$ ). We found that a single vortex is stable for the cases  $n = 1, 2$ , and  $3$  presented in Fig. 3. On the other hand, two vortices that were placed near each other show an interesting dynamics. Two singly charged vortices with the same polarity

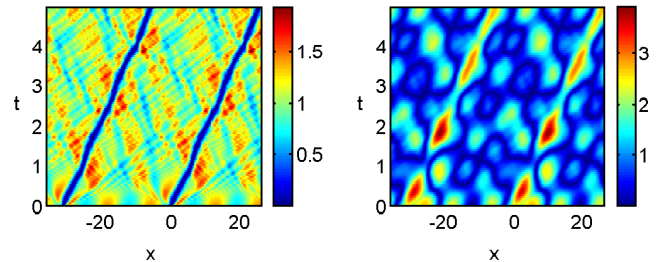


FIG. 2 (color online). The time development of the electron density  $|\Psi|^2$  (left panel) and electrostatic potential  $\varphi$  (right panel), obtained from a simulation of the system of Eqs. (1) and (2). The initial condition is  $\Psi = 0.18 + \tanh[20 \sin(x/10)] \times \exp(iKx)$ , with  $K = v_0/2A$ ,  $A = 5$ , and  $v_0 = 5$ .

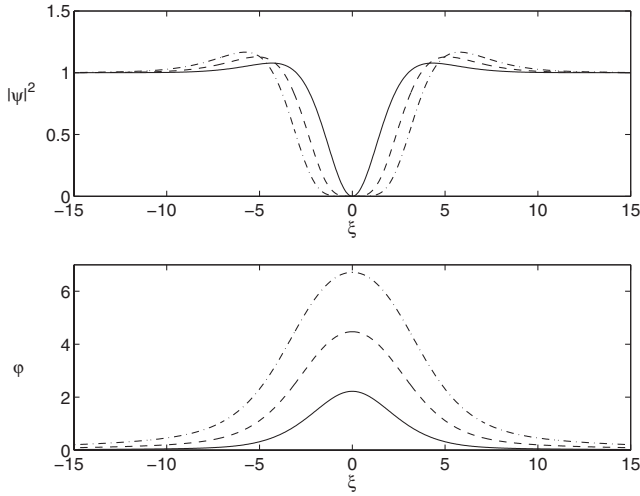


FIG. 3. The electron density  $|\Psi|^2$  (upper panel) and electrostatic potential  $\varphi$  (lower panel) associated with a two-dimensional vortex supported by the system (6) and (7), for the charge states  $n = 1$  (solid lines),  $n = 2$  (dashed lines), and  $n = 3$  (dash-dotted lines). We used  $A = 5$  in all cases.

rotate around each other, either clockwise (for  $n = 1$ ) or counterclockwise (for  $n = -1$ ) with the rotation period  $t \approx 2\pi$ , and remain stable. When the pair of vortices have opposite polarities (one having  $n = 1$  and the other  $n = -1$ ), the vortex pair also remains stable and propagates with a constant velocity in the direction of the electron flux between the two vortices. A slightly more complicated situation is illustrated in Fig. 4, where we have placed two singly charged vortex pairs at some distance from each other (see the top row), by the initial condition  $\Psi = f_1 f_2 f_3 f_4$ , where  $f_j = \tanh[\sqrt{(x-x_j)^2 + (y-y_j)^2}] \times \exp[in_j \arg(x-x_j, y-y_j)]$ . Here  $(x_1, y_1) = (-4, 10)$ ,  $(x_2, y_2) = (2, 10)$ ,  $(x_3, y_3) = (-2, -10)$ , and  $(x_4, y_4) = (4, -10)$ , and the charge states  $n_1 = +1$ ,  $n_2 = -1$ ,  $n_3 = -1$ , and  $n_4 = +1$ . The function  $\arg(x, y)$  denotes the angle between the  $x$  axis and the point  $(x, y)$ , and it takes values between  $-\pi$  and  $\pi$ . The vortices in the pairs have opposite polarity on the rotation, as seen in the electron fluid rotation direction in the upper right panel. The time development of the system exhibits that the “partners” in the vortex pairs attract each other and propagate together with a constant velocity in the direction of the electron flux between the partners. When the two vortex pairs collide and interact (see the second and third pairs of panels in Fig. 4), the vortices keep their identities and change partners in a manner of asymptotic freedom, resulting into two new vortex pairs which propagate obliquely to the original propagation direction. Two doubly charged vortices with the same polarity (both having  $n = 2$  or  $n = -2$ ) break up into two pairs of singly charged vortices that merged and reformed again in a quasiperiodic manner. If the two vortices initially had opposite polarities (one having  $n = +2$  and the other having  $n = -2$ ), we could

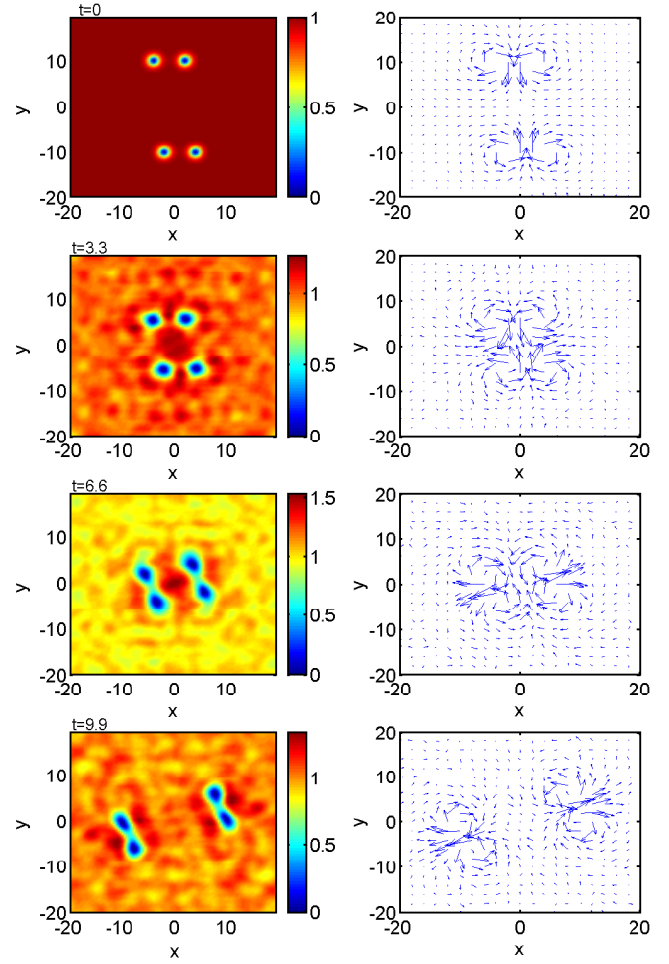


FIG. 4 (color online). The electron density  $|\Psi|^2$  (left panels) and an arrow plot of the electron current  $i(\Psi \nabla \Psi^* - \Psi^* \nabla \Psi)$  (right panels) associated with singly charged ( $n = 1$ ) two-dimensional vortices, obtained from a simulation of the time-dependent system of Eqs. (1) and (2), at times  $t = 0$ ,  $t = 3.3$ ,  $t = 6.6$ , and  $t = 9.9$  (from top to bottom). We used  $A = 5$ . The singly charged vortices form pairs and keep their identities.

observe a rapid break up of the vortex pair and the formation of quasi-one-dimensional (with larger length scale in the  $x$  than in the  $y$  direction) and long-lived dark solitons. Finally, in Fig. 5, we present 2D simulation results of Eqs. (1) and (2) with the same initial condition as in Fig. 4, except that we here used the double charge states  $n_1 = +2$ ,  $n_2 = -2$ ,  $n_3 = -2$ , and  $n_4 = +2$ . The second row of panels in Fig. 5 reveals that the vortex pairs initially move towards each other, while a quasi-one-dimensional density cavity is formed between the two vortex pairs. At a later stage, the four vortices dissolve into complicated nonlinear structures and wave turbulence. Hence, the nonlinear dynamics is very different between interacting singly and multiply charged vortices, where singly charged vortices are long-lived and keep their identities while doubly charged vortices interact in a more complicated fashion and do not keep their identities. This is, to some extent, in

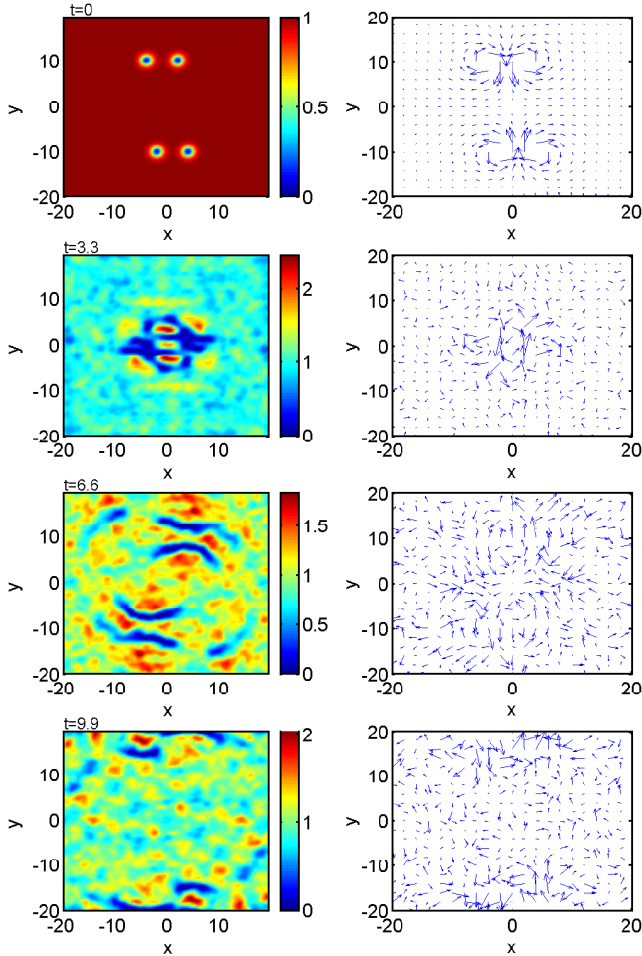


FIG. 5 (color online). The electron density  $|\Psi|^2$  (left panels) and an arrow plot of the electron current  $i(\Psi\nabla\Psi^* - \Psi^*\nabla\Psi)$  (right panels) associated with double charged ( $n = 2$ ) two-dimensional vortices, obtained from a simulation of the time-dependent system of Eqs. (1) and (2), at times  $t = 0$ ,  $t = 3.3$ ,  $t = 6.6$ , and  $t = 9.9$  (from top to bottom). We used  $A = 5$ . The doubly charged vortices dissolve into nonlinear structures and wave turbulence.

line with previous results on the nonlinear Schrödinger equation, where it was noted that vortices with high charge states are unstable [15]. In the numerical simulations of Eqs. (1) and (2), we used a pseudospectral method to approximate the  $x$  and  $y$  derivatives and a fourth-order Runge-Kutta scheme for the time stepping. The numerical simulations confirmed the conservation laws of the electron number, momentum, and energy up to the accuracy of the numerical scheme. The numerical solutions of the time-independent systems (3) and (4) as well as (6) and (7) were obtained by using the Newton method, where the  $\xi$  derivatives were approximated with a second-order centered difference scheme with appropriate boundary conditions on  $\Psi$  and  $\varphi$ .

In summary, we have demonstrated the existence of localized nonlinear structures in quantum electron plasmas. The electron dynamics in the latter is governed by a coupled nonlinear Schrödinger and Poisson system of equations, which admit a set of conserved quantities. The latter were checked numerically. Quasistationary, localized structures in the form of one-dimensional dark solitons and two-dimensional vortices were found by solving the time-independent systems of Eqs. (3) and (4) as well as (6) and (7) numerically. These structures are associated with a local depletion of the electron density associated with positive electrostatic potential and are parametrized by the quantum coupling parameter only. In the two-dimensional geometry, we have a class of vortices of different excited states (charge states) associated with a complete depletion of the electron density and an associated positive potential. Numerical simulations of the time-dependent system of Eqs. (1) and (2) show the formation of stable dark solitons in one-space dimension with an amplitude consistent with the one found from the time-independent solutions. In two-space dimensions, the quantum vortices of the first excited state were found to be stable and the preferred nonlinear state was in the form of electron vortex pairs of having different polarities. Pairs of quantum electron vortices of multiply excited states were found to be unstable. One-dimensional dark solitons and singly charged two-dimensional quantum electron vortices are thus long-lived coherent nonlinear structures, which can transport information at quantum scales in micromechanical systems and dense laboratory plasmas.

- 
- [1] P.A. Markowich *et al.*, *Semiconductor Equations* (Springer, Berlin, 1990).
  - [2] K.H. Becker, K.H. Schoenbach, and J.G. Eden, *J. Phys. D* **39**, R55 (2006).
  - [3] M. Opher *et al.*, *Phys. Plasmas* **8**, 2454 (2001).
  - [4] F. Haas, G. Manfredi, and M. Feix, *Phys. Rev. E* **62**, 2763 (2000).
  - [5] G. Manfredi and F. Haas, *Phys. Rev. B* **64**, 075316 (2001).
  - [6] D. Anderson *et al.*, *Phys. Rev. E* **65**, 046417 (2002).
  - [7] F. Haas *et al.*, *Phys. Plasmas* **10**, 3858 (2003); F. Haas, *ibid.* **12**, 062117 (2005).
  - [8] A.V. Andreev, *JETP Lett.* **72**, 238 (2000).
  - [9] G. Manfredi, quant-ph/0505004-v1.
  - [10] C.L. Gardner and C. Ringhofer, *Phys. Rev. E* **53**, 157 (1996).
  - [11] M. Loffredo and L. Morato, *Nuovo Cimento Soc. Ital. Fis.* **108B**, 205 (1993).
  - [12] R. Feynman, *Statistical Mechanics, A Set of Lectures* (Benjamin, Reading, 1972).
  - [13] A. Doms *et al.*, *Phys. Rev. Lett.* **80**, 5520 (1998).
  - [14] E.B. Kolomeisky *et al.*, *Phys. Rev. Lett.* **85**, 1146 (2000).
  - [15] I.A. Ivonin, V.P. Pavlenko, and H. Persson, *Phys. Rev. E* **60**, 492 (1999).